Urban Climate 44 (2022) 101202

Contents lists available at ScienceDirect

Urban Climate

journal homepage: www.elsevier.com/locate/uclim

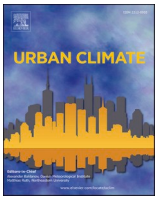

Estimation of particulate matter pollution using WRF-Chem during dust storm event over India

Manish Soni [a,e], Sunita Verma [b,c], Manoj K. Mishra [d], R.K. Mall [b,c], Swagata Payra [a,*]

[a] Department of Remote Sensing, Birla Institute of Technology Mesra, India
[b] Institute of Environment and Sustainable Development, Banaras Hindu University, Varanasi 221005, Uttar Pradesh, India
[c] DST-Mahamana Centre of Excellence in Climate Change Research, Banaras Hindu University, Varanasi, India
[d] Space Applications Centre, Indian Space Research Organisation (ISRO), Ahmedabad, India
[e] Institute for the Environment, The University of North Carolina at Chapel Hill, Chapel Hill, NC, USA

ARTICLE INFO

Keywords:
MODIS
WRF-Chem
AOD
Particulate matter
PM_{10}
AERONET

ABSTRACT

This study estimates the ground-level PM_{10} concentration by effectively combining the Aerosols Optical Depth (AOD) from Moderate Resolution Imaging Spectroradiometer (MODIS) satellite retrievals and Weather Research and Forecasting Model coupled with Chemistry (WRF-Chem). The model simulates typical dust storm events 17th-22nd April 2010 and 05th–10th May 2010 which has severely affected air quality in North and Northwestern India. The satellite retrievals shows high AOD (>1.0) over Indo Gangetic Plains and nearby Thar Desert. The model captures the spatial pattern of AOD very well however, it underestimates high aerosol loading in comparision to $MODIS_{AOD}$. The modeled AOD ($MODEL_{AOD}$) shows an underestimation by 37% with $MODIS_{AOD}$ over the study region. Therefore, the WRF-Chem model Particulate Matter (PM_{10}) and $MODEL_{AOD}$ are scaled using satellite $MODIS_{AOD}$ to provide a better estimation of the particulate pollution. The results shows better estimation, trend and correlation ($R = 0.83$) of the PM_{10} with hourly observations at Delhi monitoring station and a Mean Bias (MB) of 61 $\mu g/m^3$ during the satellite overpass time. The comparison of estimated PM with daily averaged observations of PM_{10} from Central Pollution Control Board (CPCB) at stations of Jaipur, Jodhpur, Kota, and Delhi showed a strong agreement with an correlation of (R) of 0.81, 0.70, 0.77 and 0.78, respectively.

1. Introduction

Dust storm is a common phenomenon of meteorology which happens generally during pre-monsoon season in the arid and semi-arid regions and is usually associated with hot dry air. These strong winds lift large amounts of sand and dust from bare, dry soils into the atmosphere, transporting them hundreds to thousands of kilometers away. The dust storms are a natural source of air pollution. They carry a significant amount of dust particle due to which the people suffer eye irritation, loss of visibility and other health problems etc. (e.g., Dey et al., 2004; El-Askary et al., 2006). They cover large geographical areas for deposition of different trace gases (e.g., Dentener et al., 1996; Wang et al., 2012), transportation of minerals from one place to another (e.g iron) (Jickells et al., 2005; Kalenderski et al., 2013). These dust storms can alter the cloud-aerosol properties and in turn can affect the amount of precipitation

Abbreviations: PM, Particulate Matter; RSPM, Respirable Suspended Particulate Matter; MODIS, Moderate Resolution Imaging Spectroradiometer; LU/LC, Land Use/Land Cover; AERONET, Aerosol Robotic Network.

* Corresponding author.
E-mail address: spayra@gmail.com (S. Payra).

https://doi.org/10.1016/j.uclim.2022.101202
Received 13 July 2021; Received in revised form 21 April 2022; Accepted 26 May 2022
Available online 13 June 2022

(Miller et al., 2004; Zhao et al., 2011; Teller et al., 2012, Kumar et al., 2014). Dust storm contains particles of dust or aerosols, which are removed from the atmosphere either by dry and wet deposition. These aerosols suffer dry deposition over the arid region and wet deposition over humid or moist areas like the ocean or during rainfall. The observations and simulations experiments showed that the source regions can be far distant (distance >1000 km) or from other continents and vice versa (Tegen and Fung, 1994; Ginoux et al., 2001; Prospero et al., 2002; Prospero and Lamb, 2003; Mahowald et al., 2005; Uno et al., 2006; Li et al., 2008). These dust aerosols can alter the optical properties of aerosols as well as the air quality. The harmful impacts of it occur on local to regional scale. Some of these kinds of studies are investigated in India also (e.g., Dey et al., 2004; Prasad et al., 2007; Zhao et al., 2010, 2011; Han et al., 2011; Kalenderski et al., 2013). Most of these studies are limited to validation of model outputs with ground observations (e.g., Dey et al., 2004; Chinnam et al., 2006; Hegde et al., 2007; Prasad and Singh, 2007; Prasad et al., 2007; Pandithurai et al., 2008; Sharma et al., 2012). Still, the knowledge about source and sink of dust aerosols (spatial distribution), its impact on air quality is limited over the Indian sub domain.

Around 90% of the dust emissions are emitted from arid and semi-arid regions and mostly happen in the northern part of the globe (Li et al., 2008). These fine particles are transported and deposited through the process of saltation and suspension. Over India, the source of dust storms is Great Indian Thar desert which is situated in the western part of India (Washington et al., 2003; Gautam et al., 2009). These dust storms generally happen during the pre-monsoon period when the prevailing wind blow from west or southwest, which favor the transport of dust particles from Thar desert to Northern part (Kumar et al., 2014). They have a distinct seasonal cycle, higher frequency, and intensity during the pre-monsoon period (Sikka, 1997; Dey et al., 2004; Prasad and Singh, 2007). Areas of densely populated areas are more affected due to these storm events. Some of the studies over India suggested that these dust loading events has significantly changed the optical properties of aerosols over Kanpur (Dey et al., 2004; Prasad and Singh, 2007), Delhi (Pandithurai et al., 2008), Nainital (Hegde et al., 2007). The influence of dust storms on aerosols optical properties and their impact on the energy budget has been studied using the WRF-Chem over the seven sites namely Kanpur, Jaipur, Lahore, Kathmandu, Pokhara, Nanital and EVK2-CNR covering both urban conditions as well as cleaner high-altitude sites (Kumar et al., 2014).

The studies related to PM spatio-temporal variability and the assessment through models is highly uncertain and limited due to sparse availability of PM ground-based observations in India. The AOD values retrieved from satellite based instruments are recently been used to derive surface PM concentrations. Different methodologies, such as statistical models or neural networks, to estimate PM has been used. However, research on PM_{10} estimation using a combination of ground-measured, satellite-estimated, and atmospheric chemical model are limited The present research paper is focused on the application of Weather Research and Forecasting Model coupled with Chemistry (WRF-Chem) to simulate typical pre-monsoon dust events and estimate PM_{10} pollution over Northern India. The previous studies by Kumar et al. (2012a, 2012b), Ghude et al., 2013 suggests WRF-Chem model is capable to simulate the important features of meteorology, chemistry over Indian region. The previous WRF-Chem results depicts that modeled PM is significantly underestimated (Govardhan et al., 2015; Crippa et al., 2016). This paper thus uses a scaling method to estimate PM using combined use of satellite-based AOD retrievals along with model generated PM_{10} and AOD to estimate the particulate pollution over Rajasthan and Delhi. The validation of model results against the ground observations (Hourly or daily) taken from Central Pollution Control board (CPCB) (https://app.cpcbccr.com/ccr/#/caaqm-dashboard/caaqm-landing) has also been carried out.

The manuscript is divided into four sections. Section 2 covers the model domain and detailed configuration. Section 3 describes the observational datasets of AERONET for validation of the MODIS satellite retrievals. It also provides information about sites and CPCB

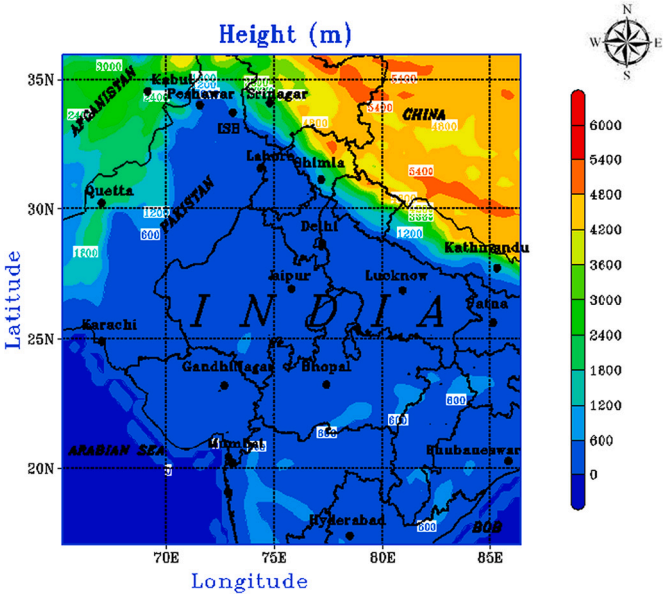

Fig. 1. Model Domain for present study.

PM_{10} datasets. Section 4 gives the details on the results and discusses in detail. Section 5 contains the summary from the findings.

2. The WRF-Chem model

2.1. General description WRF model

The present work utilizes the WRF model, a next-generation mesoscale model with the capability to run with and without nesting. The model is developed primarily at the National Center for Atmospheric Research (NCAR) in collaboration with different agencies like the National Oceanic and Atmospheric Administration (NOAA), the National Center for Environmental Prediction (NCEP), and many others. The WRF is a limited-area, non-hydrostatic, primitive-equation model with multiple options for various physical parameterization schemes (Skamarock et al., 2008). It uses the Arakawa C horizontal grid along with Runga Kutta third order time integration scheme. The model follows the terrain and conserves the scalar variables.

Different physics options are available in the model that can be used as per need. It is very essential to run different simulation schemes to find out the better combination for a particular location.

2.2. Description of WRF-Chem model

This study uses version 3.6.1 of the Weather Research and Forecasting Model (Skamarock et al., 2008) coupled with Chemistry (Grell et al., 2005; Fast et al., 2006) to simulate the meteorology and chemistry over the model domain shown in Fig. 1. The projection of the domain is Mercator. The single domain covers 80 × 80 grid points in north-south and east west direction at 27 km × 27 km grid resolution (Fig. 1). The default geographical static fields such as soil properties, terrain height, vegetation fraction, dust erosion, land use etc. are interpolated at 10 mins (~19 km) taken from United States Geographical Survey (USGS) data using WRF preprocessing system (WPS). We have also used the updated LU/LC of India for 2010 taken from bhuvan portal under National Information center for Environmental and Climate Sciences (NICES)) theme at 5 min resolution from IRS-P6 AWiFS (Gharai et al., 2018). It has 25 LU/LC categories with 56 min spatial resolution scaled to 5,2 min and 30 s resolution. These are accurate and updated on annual basis from 2004 to 05 to 2018–19. This is done by replacing the default USGS data with AWiFS derived compatible WRF input data. This domain covers the higher Himalayas, Plain areas of Indo Gangetic Plains, Thar desert and parts of Arabian Sea and Bay of Bengal. The meteorology and atmospheric chemistry are hugely affected by this undulating surface with varying heights.

2.3. Physical parameterization

The physical parameterization options used in the study are described below:

1) Microphysics (mp_physics = 8 i.e., Thompson microphysics scheme (Thompson et al., 2004))

This scheme is particularly useful for high-resolution simulations. It is a particularly new scheme which accounts for ice snow and graupel processes and adds rain number concentration.

2) Surface Layer Parameterization (sf_sfclay_physics = 1 i.e., Revised MM5 similarity scheme (Beljaars, 1994))

This surface layer scheme is based upon Monin-Obukhov and Carlson-Boland theory of viscous sub-layer processes and standard similarity functions.

3) Land Surface Parameterization (sf_surface_physics = 2 i.e. NOAH Land Surface model (Chen and Dudhia, 2001))

This scheme gives multiple options for important atmosphere interactions processes.

4) Planetary Boundary Layer Parameterization (bl_bpl_physics = 1 i.e. Yonsei University (YSU) boundary layer scheme (Hong et al., 2006))

It is a nonlocal scheme and contains explicit entrainment layer and parabolic profile layer for particularly unstable mixed layer environment.

5) Cumulus Parameterization (cu_physics = 1 i.e., Kain–Fritsch convective scheme (Kain, 2004))

This scheme accounts for deep and shallow convection subgrid cloud effects using mass flux approach. This scheme also interacts well with radiation.

6) Radiation Scheme

a) Longwave radiation (ra_lw_physics =4 i.e. Modified Rapid Radiative Transfer Model (RRTM) Mlawer et al., 1997)

This long wave scheme is particularly useful for multiple bands, trace gases and microphysics species and accounts for random cloud overlap.

b) Shortwave radiation (ra_sw_physics =4 i.e., Modified Rapid Radiative Transfer Model (RRTM) Mlawer et al., 1997)
This scheme accounts for random cloud overlap.

2.4. Chemistry

The WRF-Chem simulation considers the inclusion of emissions as well as chemistry initial and boundary conditions. The anthropogenic emissions of CH_4, NMVOC, CO, SO_2, NO_x, NH_3, PM_{10}, $PM_{2.5}$, BC, and OC are taken from the emission database for global atmospheric research (EDGAR). This EDGAR-HTAP V2 emission database is at $0.1^\circ \times 0.1^\circ$ spatial resolution (Janssens-Maenhout et al., 2012). It contains monthly and annual grid split-up maps of the sector-specific global emissions of the year 2010. Anthro_emiss tool is used for providing the daily emissions for mapping to MOZART-MOSAIC and MOZART-GOCART chemical options. Residential biomass burning is included in anthropogenic emissions. Open biomass burning fire emission is obtained from the Fire Inventory from NCAR version 1 (FINN v1) (Wiedinmyer et al., 2011). It produces daily emission estimates of biomass burning at a horizontal resolution of ~1 km^2. Model of Emissions of Gases and Aerosols from Nature (MEGAN) version 2.04 is used to calculate online biogenic emissions of trace gases (Guenther et al., 2006). Only aerosol direct effects (Scattering and Absorption) are considered. The aerosol processes and gas phase chemistry are represented by Goddard Chemistry Aerosol Radiation and Transport (GOCART) bulk aerosol scheme (Chin et al., 2002; Pfister et al., 2011) and MOZART-4, known as MOZCART (MOZART+GOCART). More information about the aerosol modules can be found at https://ruc.noaa.gov/wrf/wrf-chem/users_guide.pdf. Dust in WRF-Chem is divided into 5 size bins. The radii of these bins are 0–1 (bin1), 1–1.8 (bin2), 1.8–3 (bin3), 3–6 (bin4) and 6–10 (bin5) μm. $PM_{2.5}$ concentration is total of bin1 along with 0.31 times of bin2. PM_{10} concentration is total of the first three bins (bin1 + bin2 + bin3) along with 0.87 times of bin4. This is more deeply explained in module 'gocart_aerosols.F' of chemistry module. Firstly, the meteorological data is processed by WRF-Preprocessing System (WPS), input emissions are processed by emission tools utilities (Anthropogenic, Fire, Biogenic). Together they provide input for real data initialization, updation of chemical initial and boundary conditions and WRF. The output from WRF-Chem is then post processed through Advance Research WRF Post Processing (ARWpost) and visualized using Grid Analysis and Display System (GRADS).

3. Data collection and methodology

3.1. Satellite data

The Level 3.0 collection version 6.1 AOD at 550 nm wavelengths is extracted from MODIS satellite Terra (10:30 h) and Aqua (13:30 h) platform for the study period. This is earth-gridded averaged daily geophysical parameter data and is a combined product of dark target and deep blue AOD under cloud-free conditions. For spatial filtration, bad pixels having AOD value −9999 are masked out. Then, it is used for the estimation of PM_{10}.

For point data estimation, Firstly, bad pixels (having value −9999) and outliers were removed and then those pixels which lie within the mean ± standard deviation are taken. The spatial window size of ±0.25 of latitude and longitude (Payra et al., 2015) around validation sites is taken wherever ground stations of AERONET camel sun photometer are there.

The previous study by Payra et al., 2015 suggested a bias in satellite $MODIS_{AOD}$ over Jaipur, Gual Pahari (Close to Delhi), Pune and Kanpur with respect to ground observations of $AERONET_{AOD}$ with values in range of $+0.06 \pm 0.24$, 0.10 ± 0.14, 0.30 ± 0.23 and 0.09 ± 0.14, respectively.

For daily estimation, both combined product of (Dark Target and Deep Blue) of Terra and Aqua AOD retrievals are used. In the same way, while during hourly estimation wherever PM_{10} hourly observations are available both Terra and Aqua are used separately.

3.2. Particulate matter data

Daily Particulate matter (PM_{10}) of size less than or equal to 10-μm meter has been measured with particulate sampler installed by Rajasthan Pollution Control Board (RPCB) over Jaipur at six stations namely at Ajmeri Gate, Board Office Jhalana Dungri, Chand Pole, Malviya Industrial Area (MIA), RO Vidhyadhar Nagar, Viswakarma Industrial Area (VKIA). We have taken MIA station RSPM data as it is nearest to the weather station as well as AERONET station (distance less than 10 km). The unit of RSPM is microgram per meter cube.

For Jodhpur, the daily values of RSPM are taken from https://data.gov.in/ provided by CPCB (Soni et al., 2018). CPCB has monitoring stations at Basni Industrial Area, Housing Board Office Chopasani Road, DIC office, Maha Mandir Police Thane, Shastri Nagar Police Thane and Sojati Gate. Same way data is taken for Alwar and Kota district where there are 3 monitoring stations. All the data is merged since all the locations are within 10 km of the meteorological station.

For Delhi, during the simulation period hourly and daily values are taken from Dwarka Monitoring station of Central Pollution Control Board.

3.3. AIRS dust score

Aqua satellite orbiting around Earth also has an Atmospheric Infrared Sounder (AIRS) when used Advanced Microwave Sounding

Unit (AMSU), provides 3D look at Earth's weather and climate by emitting infrared and microwave radiations (AIRS Science Team/ Joao Teixeira (2013)). Together, AIRS provide data that can improve the weather forecasting as well as improving our knowledge of Earth Climate complexity. It works in tandem and have more than 2000 channels. It provides 3D maps of temperature and humidity, cloud amounts and heights, greenhouse gas concentrations and many other atmospheric phenomena and managed by NASA's Jet Propulsion Laboratory in Pasadena, California (Yao et al., 2019). The instrument takes data daily at 01:30 am and 01:30 pm daily at local time. The Level 2 data is taken at cloud free conditions in HDF-EOS format. The data is available at 50 km spatial resolution at nadir. It has a temporal resolution of 6 min taking 240 granules per day. Aqua/AIRS Level 2.0 Support Retrieval (AIRS-only) V6.0 (AIRS2SUP) contains the data field dust_score which provides score indicating more certainty of dust (https://disc.gsfc.nasa.gov/datasets/AIRS2SUP_006/summary). Dust is more probable when dust score > 380. This score is valid only when dust flag is positive. We have analyzed the dust score data during simulation period (14 April- 14 May 2010).

3.4. Data methodology

3.4.1. Aerosol optical depth

Aerosol optical properties are available at 4 wavelengths (i.e., 300,400,600,999 nm) in WRF-Chem. The Fortran routine for aerosols computes optical properties at these discrete wavelengths for short wave radiation. This range of spectrum (especially visible) covers both fine and coarse particles and any AOD values can be interpolated or extrapolated using power law and AE. Higher wavelength greater than 900 nm are responsible for water vapor. AOD 550 nm lies in the middle of visible spectrum and the value can be interpolated using $AE_{400–600\ nm}$. This is done because AE obtained from satellite retrievals are closer for $\lambda_1 = 400$ and $\lambda_2 = 600$ nm (Kumar et al., 2014; Crippa et al., 2016).

To match $MODIS_{AOD}$ retrievals wavelength $MODEL_{AOD}$ from WRF-Chem is converted to similar wavelength using power-law function as described in Eqs. (1) and (2) (Eck et al., 2001).

$$\alpha = -\frac{ln\left(\frac{AOD_{400}}{AOD_{600}}\right)}{ln\left(\frac{\lambda_1=400}{\lambda_2=600}\right)} \tag{1}$$

$$MODEL_{AOD} = AOD_{600} \times \left(\frac{\lambda_1}{\lambda_2}\right)^{-\alpha} \tag{2}$$

Where,

a denotes Angstrom Exponent, $AOD_{400,}$ AOD_{600} denotes model AOD at wavelength 400(λ_1) and 600(λ_2) nm. $MODEL_{AOD}$ is the derived model AOD at 550 nm of WRF-Chem using power law.

3.4.2. Estimation of Particulate Matter (PM_{10}) using model and satellite AOD

Due to the scarcity of ground monitoring of particulate matter, special techniques are used nowadays to estimate PM. The main advantage of using satellite data is wide spatial and temporal coverage. (Lee et al., 2011; Chitranshi et al., 2015; Park et al., 2014, Kim et al., 2016, Payra et al., 2015). Estimation of PM is generally done using aerosol optical depth (AOD).

$$AOD = \int_0^\infty \sigma_{ext}(h)dh \tag{3}$$

Where σ_{ext} is extinction coefficient of aerosols at height H.

The particulate concentration at surface level is measured by ground-based monitors (Zhang et al., 2017). The AOD (unitless) and PM ($\mu g/m^3$) can be correlated by following equation shown in Eq. (4) (Koelemeijer et al., 2006; Gupta and Christopher, 2009; Hoff and Christopher, 2009; Sotoudeheian and Arhami, 2014; Soni et al., 2018). Both of these parameters (AOD and PM) describe air quality and atmospheric condition.

$$\mathrm{AOD} = \mathrm{PM} \times \mathrm{H} \times \mathrm{f(RH)} \frac{3\ \mathrm{Q}_{ext,\mathrm{dry}}}{4\ \rho \mathrm{r}_{\mathrm{eff}}} = \mathrm{PM} \times \mathrm{H} \times \mathrm{S} \tag{4}$$

Where, ρ is aerosol mass density ($g\ m^{-3}$), f (RH) is the ratio of ambient and dry extinction coefficients (size distribution integrated), $Q_{ext,\ dry}$ is the Mie extinction efficiency,

H is the boundary layer height and r_{eff} is the particle effective radius (dependent on size distribution). S is the specific extinction efficiency ($m^2\ g^{-1}$) of the aerosol at ambient relative humidity (RH).

The Eq. (4) is used under cloud-free skies when aerosols are well confined within the boundary layer. The relationship between these two depends on the size distribution, particle composition and vertical profile of aerosols.

The ratio of PM with AOD is better provided by atmospheric chemistry model due to the scarcity of ground stations at every spatial point. These models can be used to predict PM which includes the meteorology, chemistry and dispersions(Liu et al., 2004; Gupta et al., 2006; Van Donkelaar et al., 2006, 2010; Li et al., 2015; Bilal et al., 2017). However, the results obtained contains uncertainity due to updated emission inventories, dynamical processes as well chemical process of aerosols in atmosphere (Chate and Devara, 2005; Kondragunta et al., 2008; Gupta and Christopher, 2009; Lin et al., 2015).

These kind of uncertainities can be removed considerably by using satellite retrieved AOD as a scaling factor. We know that MODIS

Terra and Aqua satellite AOD retrievals are providing us long-term quality-assured data at 10:30 and 13:30 locally under cloud free conditions(Kaufman et al., 1997; Chu et al., 2002; Remer et al., 2005; Levy et al., 2007; Lee et al., 2011; Dey et al., 2012; Yap and Hashim, 2013; Song et al., 2014; Payra et al., 2015; Soni et al., 2018). These retrievals can be used as a scaling factor to calibrate the Modeled PM and AOD ratio (Liu et al., 2004; Van Donkelaar et al., 2006; Liu et al., 2007; Krishna et al., 2019).

$$EstimatedPM_{10} = \frac{MODELPM_{10}}{MODEL_{AOD}} \times MODIS_{AOD} \quad (5)$$

Throughout the paper, this method is used to estimate the PM_{10} (Estimated PM_{10}) using daily and hourly collocated observations (Eq. (5)).

4. Results and discussion

As a first step, the WRF-Chem model run has been performed for single domain at 27 km × 27 km grid resolution (Fig. 1) for a time period from 14th April 2010 to 14th May 2010 with integration every 1 h over the selected Indian domain with spin up time of 2 days. The detailed model configurations have been described in Section 2.1.

The results primarily focus on the evaluation of the model performance for aerosols optical depths. In this section, model simulated AOD are analyzed. Later, the model results were evaluated against observations at few monitoring sites.

4.1. Validation of model AOD

The Fig. 2 shows the averaged $MODIS_{AOD}$ and mean bias (MODIS retrieved AOD and WRF-Chem simulated AOD) during the peak dust storm event from 17th-22nd April 2010. $MODIS_{AOD}$ data represents the true image of air quality and atmospheric condition for the peak dust storm period (i.e 17th-22nd April 2010). The spatial distribution of AOD shows peak of AOD over North and Northwestern India during the dust episode of 17th–22nd April 2010. In North India, especially the Indo Gangetic Plain (IGP) shows high aerosol optical depth. The model is able to capture the general spatial pattern as the satelite AOD. However, the $Model_{AOD}$ (0.6–0.8) is underestimated in comparision to $MODIS_{AOD}$ (0.8–1.0) over IGP. During the peak dust storm period of pre-monsoon (17th-22nd April 2010), the mean difference of 0.11 ± 0.18 has been found out between the $MODIS_{AOD}$ and $Model_{AOD}$. The minimum bias was −0.34 and maximum was 0.94. WRF-Chem simulated modeled AOD was found underestimated at high sources of aerosol loading i.e. North-West and IGP regions. The mean bias graph (Fig. 2, RHS) shows the difference of 0.4–0.8 at dust affected areas. The red color in mean bias shows overestimation and blue shows underestimation.

The results shows that WRF-Chem underestimate AOD by almost 43% when compared with $MODIS_{AOD}$ during the first peak i.e. 17th -22nd April 2010. Fig. 2 also shows underestimation of AOD over IGP and Northwest India which implies underestimation of pollution also. The AOD and AE area averaged is shown in Fig. S1 of supplemenatry information suggesting the domiance of natural source of pollution during the simulation period.

The WRF-Chem modeled $MODEL_{AOD}$ is also compared with satellite $MODIS_{AOD}$ at few major cities in North and Northwestern India (Table 1). The collocated observations within satellite overpass time (i.e. ±0.5 h) are compared.

The Table 1 shows the comparison of $MODIS_{AOD}$ with $MODEL_{AOD}$ at 550 nm at Delhi, Jaipur, Jodhpur and Kota. The correlation between $MODIS_{AOD}$ and MODEL PM_{10} with $MODEL_{AOD}$ comes as 0.24 and 0.75 respectively. It is clearly seen from the Table 1 that AOD obtained from the model output is generally underestimated at all stations. Model outputs of AOD at Jaipur, Jodhpur, Kota, and Delhi are generally underestimated with MODIS satellite AOD retrievals by around 37% for the whole simulation period. The observed underestimation lies well with the study done by Kumar et al. (2014) and Krishna et al. (2019). Regression analysis was performed to find the relationship between $MODIS_{AOD}$ and MODEL PM_{10} with $MODEL_{AOD}$. It is shown in Table 2.

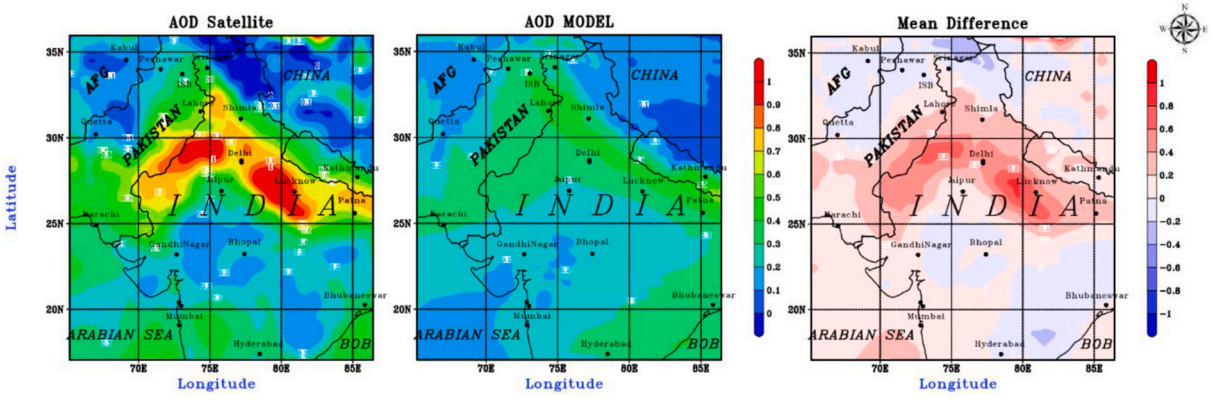

Fig. 2. Spatial comparison of $MODIS_{AOD}$ with $MODEL_{AOD}$ at 550 nm and Mean Difference ($MODIS_{AOD}$ minus $MODEL_{AOD}$) during the peak dust storm event from 17th-22nd April 2010.

Table 1
Comparison of $MODIS_{AOD}$ with $MODEL_{AOD}$ at 550 nm at Delhi, Jaipur, Jodhpur and Kota location.

Site Location	$MODIS_{AOD}$ 550 nm	$MODEL_{AOD}$550 nm
Delhi	0.65 ± 0.20	0.49 ± 0.23
Jaipur	0.38 ± 0.28	0.30 ± 0.20
Jodhpur	0.57 ± 0.34	0.19 ± 0.16
Kota	0.37 ± 0.12	0.22 ± 0.16

4.2. Scaling $MODEL_{AOD}$ and PM_{10}

As seen from Section 4.1 $MODEL_{AOD}$ is very much underestimated. We have tried to find out the reason for underestimation. This can be better seen during the peak event i.e. on 21st April and 8th May 2010. The average Planetary Boundary layer (PBL) height during the daytime ranges from around 1500–3500 m which is shown in Fig. 3. For the particular event the average PBL height near Delhi, Jaipur, Indo Gangetic plain is in range of around 2500–3500 m. When PBL height is more there is more turbulence and aerosols are transported to far distant places. Also, below this layer all significant exchange of momentum, flux, wind velocity takes place.

In Fig. 3, LHS, the direction is from Thar desert towards IGP then downwards states like Madhya Pradesh, Telangana, and Orissa. For the RHS Figure, the wind direction is mostly towards Rajasthan and Madhya Pradesh mainly. The PBL height and surface windspeed from the model is compared with MERRA 2 Version 5 (GEOS-5) with its Atmospheric Data Assimilation System (ADAS), version 5.12.4 planetary boundary height and wind data. The comparison shows that the model systematically overestimate the planetry boundary layer height as well as surface winds (northward-eastward direction). This causes a well deeper mixing and dispersion. This causes a lower surface concentration of aerosols. These results are similar with the study done by Goverdhan et al., 2015.

4.3. PM estimation using scaling method ($MODIS_{AOD}$)

As the model results depict a significant underestimation of AOD as seen from Sections 4.1 and 4.2. MODIS Terra and Aqua satellite AOD retrievals are used as a scaling factor to improvise PM estimation. The MODIS provide long-term quality-assured data at 10:30 and 13:30 locally. These retrivals are used as a scaling factor to calibrate the Modeled PM and AOD ratio (Liu et al., 2005). The details of scaling method has been given in Section 3. The PM_{10} has been estimated using Eq. (5) within ±00:30 h of satellite overpass time.

The estimated PM using Eq. (5) scaling method has been further evaluated and compared with satelited and observed AOD. The Fig. 4 compares estimated PM with MODIS Aqua and Terra for 21st April 2010 while Fig. 5 compares the estimated PM with MODIS Aqua and Teraa for 8th May 2010.

4.3.1. Estimated PM vs MODIS AOD during dust stroms

The maximum spatial correlation for $MODIS_{AOD}$ and estimated PM_{10} using both Terra and Aqua is found at 11:00 am and 02:00 pm i.e. 0.58 and 0.60 during the study period 17th-22nd April 2010 and 05th-10th May 2010 respectively. In the same way minimum spatial correlation for $MODIS_{AOD}$ and estimated PM_{10} using Terra and Aqua satellite is found at 10:00 am and 01:00 pm i.e. 0.26 and 0.35 during the study period 17th-22nd April 2010 and 05th–10th May 2010 at 02:00 pm. Also, satellite $MODIS_{AOD}$ matches with Estimated PM_{10} as shown in Figs. 4 and 5 for Terra and aqua during the peak period of dust storm i.e. on 21st April 2010 and 08th May 2010. Fig. 3 shows higher AOD at the northwestern part of India as well as Indo Gangetic Plains. The spatial feature is well captured by the estimated PM_{10} on 21st April 2010. Fig. 5 shows the comparison of MODIS AOD with estimated PM_{10} after satellite overpass time on 08th May 2010. The figure shows the dominance of high AOD over north-west India only. This is also well captured by the estimated PM_{10} on 08th May 2010. MODIS Terra and Aqua satellite observation show high increase in aerosol loading resulting into increase in AOD mainly over IGP region and Thar desert (Kumar et al., 2012a, 2012b). It is well captured by dust storm events (i.e 21st April 2010 and 08th May 2010) by both satellite and model estimation over IGP and Thar desert. During this time, North West India (Red color in the map), as well as Indo-Gangetic Plains (IGP), suffers high PM_{10} episode ranging more than 600 $\mu g/m^3$. The state of the air quality is severe as per National Ambient Air Quality Standards(NAAQS), India. In all the Figs. 4 and 5 the red color in the legend specifies a highly affected area. The magnitude of this color is above 400 micrograms/m^3 which according to NAAQs comes the severe quality of air pollution.

4.3.2. Estimated PM vs ground observations

To validate the model results further the estimated PM values are compared with the ground observations. The Particulate Matter (PM_{10}) measurements are taken from the Central pollution Control Board (CPCB) for validation against the estimated PM_{10} from 14th

Table 2
Linear regression analysis to show the dependency of $MODIS_{AOD}$ and MODEL PM_{10} with $MODEL_{AOD}$.

Regression analysis	Linear regression equation and correlation
$MODIS_{AOD}$ Vs $MODEL_{AOD}$	$MODIS_{AOD} = 0.28\times MODEL_{AOD} + 0.43$ (Constant) $R = 0.24$
MODEL PM_{10} Vs $MODEL_{AOD}$	MODEL $PM_{10} = 189.45 \times MODEL_{AOD} + 48.57$ (Constant) $R = 0.75$

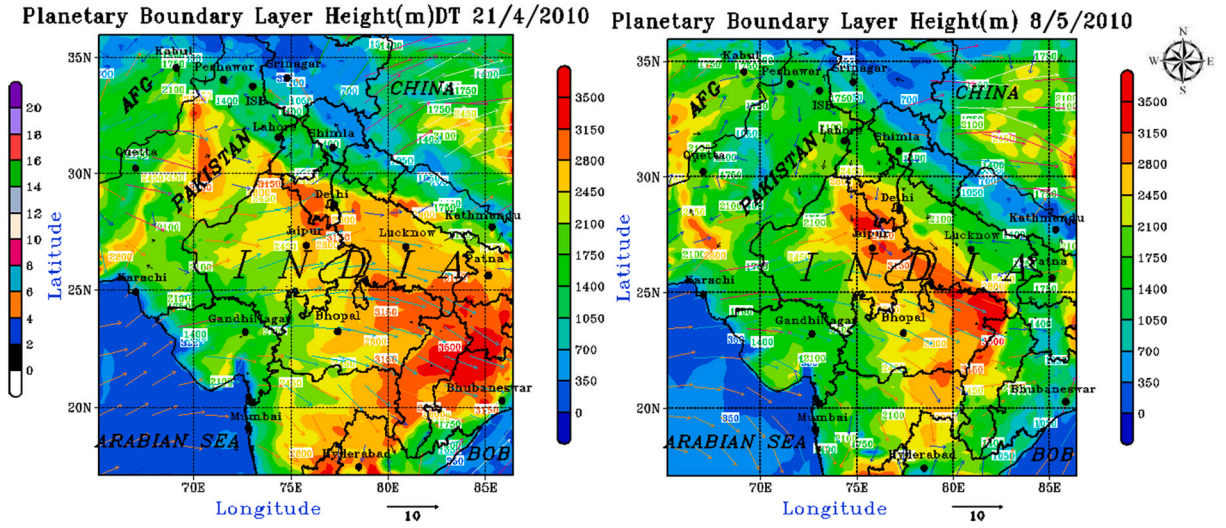

Fig. 3. WRF simulated Planetary Boundary layer (PBL) height during the daytime (09:00 am to 05:00 pm) for both events on 21st April 2010 and 08th May 2010. The color bar on the right denotes height in meters.

April 2010 to 14th May 2010. The daily measurement is available for Jaipur, Jodhpur, Kota, and Delhi during the study period. MODIS overpass time is 10:30 am and 01:30 pm (or 13:30 h) for Terra and Aqua respectively. Average combined daily estimated values of Terra and Aqua are taken to be validated against the known locations specified above. Fig. 6 given below shows the time series graph for the simulation period. For comparison we have averaged pixels of model output close to observation sites.

As seen from Section 4.1, $MODEL_{AOD}$ output is underestimated by 37% at all four locations taken together during the simulation period. By Eq. (5), if $MODEL_{AOD}$ is underestimated it will make denominator small. The numerator will be more and with adjustment of $MODIS_{AOD}$, Estimated PM_{10} some times overestimates the observed values. Whenever the $MODEL_{AOD}$ is less than 0.10 it gives more error or overestimation. For such cases, the $MODEL_{AOD}$ is multipled by factor of 5 to show much reliastic results.

The Fig. 6 shows the estimated PM_{10} has successfully captured the trend at all the four locations. The correlation for Jaipur, Jodhpur, Kota, and Delhi are 0.81, 0.70, 0.77 and 0.78 respectively. The combined correlation comes as 0.73. The slope, intecept, *p*-value and R^2 are presented in Table 3.

Jaipur is more affected by the severe PM_{10} episode of May (Figs. 4 and 5) as shown by peaks in line plot (Fig. 6) in comparision to April dust strom. Jodhpur is in a south-west direction from Jaipur. From the Figs. 6, it is clearly visible that dust strom has affected Jodhpur as its location in the vicinity of Thar Desert. Kota is in a south direction from Jaipur and it is least affected with the average PM_{10} values comes in the category of 150–200 both from observed as well as estimated. Correlation, Normalised mean square error (NMSE), Factor of two obeservations (FA2) and Fractional bias (FB) for all the merged data (taking all station data together) is 0.72, 0.56, 75 and − 0.31 respectively. The detailed information and formulas about the statistial measures used in the study are shown in Table S1 of supplementary information. Overall, the statistical results suggests that estimated PM_{10} represents the surface PM_{10} fairly at CPCB monitoring sites.

The estimated PM_{10} were also compared with the hourly observations at Delhi monitoring PM_{10} station. Fig. 6 shows the hourly validation at Delhi Dwarka station. Since CPCB gives hourly observations. The Estimated PM_{10} of 11:00 am and 02:00 pm is matched with ground observations in Fig. 7.

Fig. 7 clearly depicts that the model successfully capture the trend as well as peak values. The correlation, NMSE, FA2 and FB were 0.83,0.50,68.30,-0.40 respectively between the observations and estimated PM_{10} values. Also, from the Fig. 4(a) and (b) it can be seen that dust storm has affected the Delhi region. The first peak is seen during the simulation period 17th-22ndApril 2010. However, the dust storm or high PM episode happened during 05th–10th May 2010 has a very little effect over Delhi. So, there is no sharp peak at the end of the line plot (Fig. 7). Though, PM_{10} values were still higher than NAAQS standards.

The point data validation of estimated PM suggested that the events are well correlated and able to capture the trend with CPCB observations of PM_{10}. The status of air quality during these events vary from moderately polluted to severe. If prolonged this can cause serious health impacts and increase mortality.

4.4. Estimation of total pollution load during peak event

Fig. 8(a) shows that the wind direction is from Arabian Sea to thar desert then towards the Indo Gangetic Plains. In Fig. 8(b), the wind direction from Arabian Sea to Thar desert and is more focussed towards Jaipur, Delhi and its surroundings. From the same figure, the wind direction from IGP region is towards Delhi and Jaipur. This created a compound event. So, PM_{10} is staggered over Western India. This is the reason for high PM towards Indo Gangetic Plains while estimating PM_{10} during the 17th-22nd April 2010 dust storm event. The pathways of this dust storms is also validated using Hybrid Single-Particle Langrangian Integrated Trajectory (HYSPLIT)

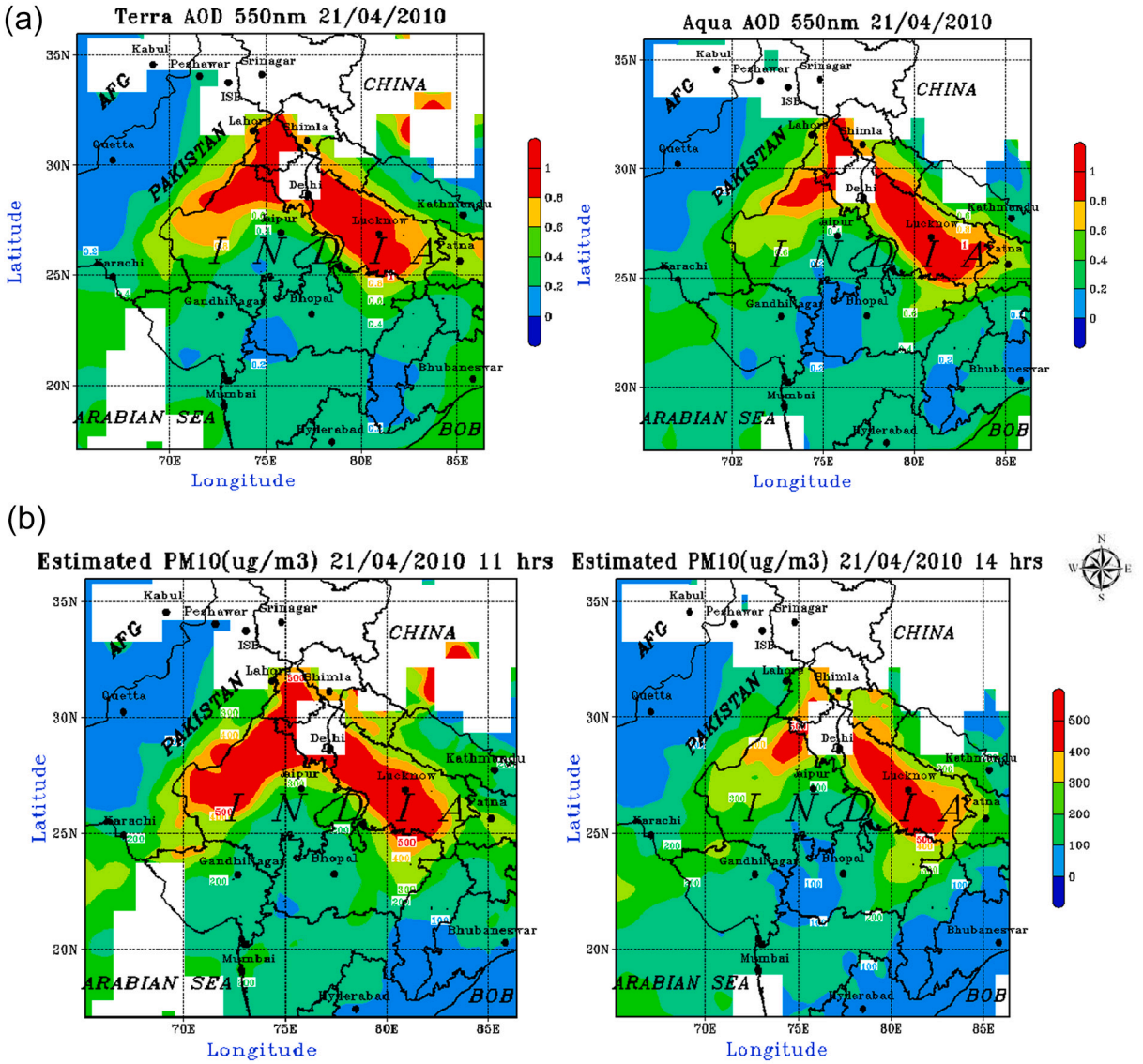

Fig. 4. a: (i, ii) MODIS Terra and Aqua AOD (unitless) on 21st April 2010 at 10:30 a.m. and 01:30 pm. b: (i, ii) Estimated PM_{10} on 21st April 2010 at 11:00 am and 02:00 p.m. after Terra and Aqua satellite overpass time.

model. This model is used to compute backward air-mass back trajectories during extreme i.e. 21st April 2010 and 08th May 2010. The trajectories were computed for the past 72 h (3 days) initialised at 06:00 h UTC over 1000 m, and 2000 m AGL in order to identify the source of local and long-range transported dust. The sink location taken is Lucknow of Indo-Gangetic Plain (IGP) to identify the pathways. Trajectory Analysis clearly shows the two dust's storm follows two different path over India. First one reached to Delhi without passing through Jaipur where the second one has passed through Jaipur. Ground observation also validate this. The long-range dust transport came from Arabian Peninsula and Middle East, contributing to the high pollution event during these dusty days. The results are similar with the study done by Chinnam et al., 2006; Moorthy et al., 2007; Satheesh and Srinivasan, 2002, Sharma et al., 2012 where they have idenfied the same source and sinks during pre-monsoon dust storms. This is added as Fig. S2 in supplementary information.

4.5. Dust scores load during peak event

We have analyzed the dust score (>380) during peak dust event i.e. on 20th and 21st April 2010 as shown in Fig. 9 using the composite image (day and night). The first Fig. 9(a) shows dust proximity and certainity more severe over Northwest part of India specially west of Rajasthan, Delhi, parts of Punjab, IGP region on 20th April 2010. This regions conincides with the high AOD regions and PM_{10} regions discussed in 4.3.1. The second figure i.e. Fig. 9(b) shows how the dust is transporated towards IGP, Rajasthan the

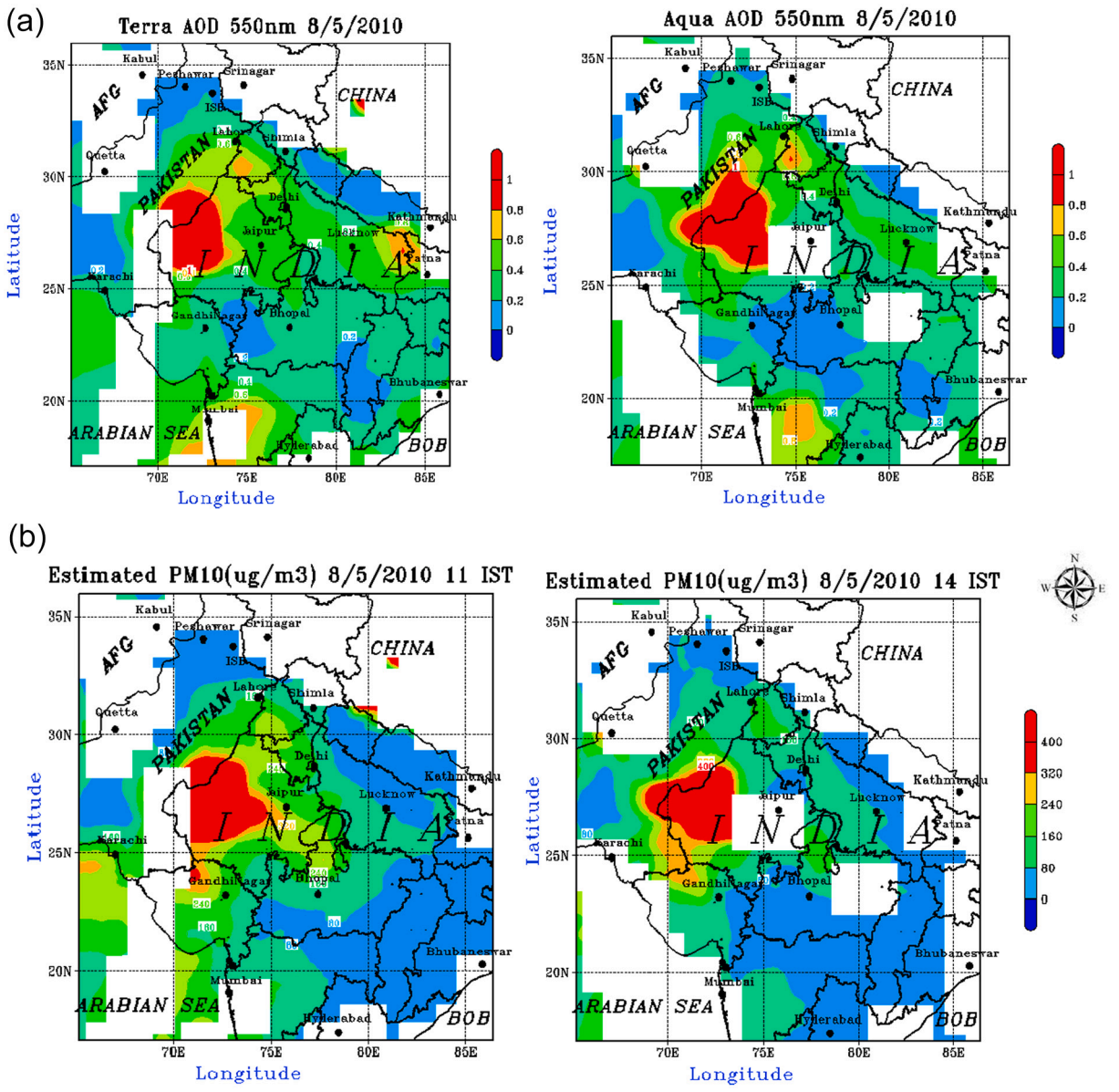

Fig. 5. a: (i, ii) MODIS Terra and Aqua AOD (unitless) on 08th May 2010 at 10:30 a.m. and 01:30 pm. b: (i, ii) Estimated PM_{10} on 08th May 2010 at 11:00 am and 02:00 p.m. after Terra and Aqua satellite overpass time.

very next day.

We have analyzed the dust score (>380) during peak dust event i.e. on 03th May 2010 as shown in Fig. 10 using the composite image (day and night). This was a much local event affecting mostly Rajasthan, some parts of Delhi. The dust is dispersed and setttled also very quickly. As seen from Fig. 8(b) the wind direction is centering along and towards rajasthan only. This event hasn't affected other parts of India.

5. Summary and conclusions

This study uses the WRF-Chem model to simulate typical pre-monsoon dust events which has affected North-West and Indo Gangetic plains, India. The WRF-Chem model PM_{10} and $MODEL_{AOD}$ are scaled through $MODIS_{AOD}$ (satellite observations) to provide a better estimate of the particulate pollution. It has been seen in the study that natural source of pollution i.e. dust storm during the 17th-22nd April 2010 has affected entire Northern India and dust storm during 05th-10th May 2010 has affected mainly North-West India. MODIS Terra and Aqua AOD retrievals during the simulation period shows high AOD nearby Thar Desert and Indo Gangetic Plains which reached extreme on 21st April 2010 and 05th–08th May 2010. The estimated PM_{10} has well captured these events and showed

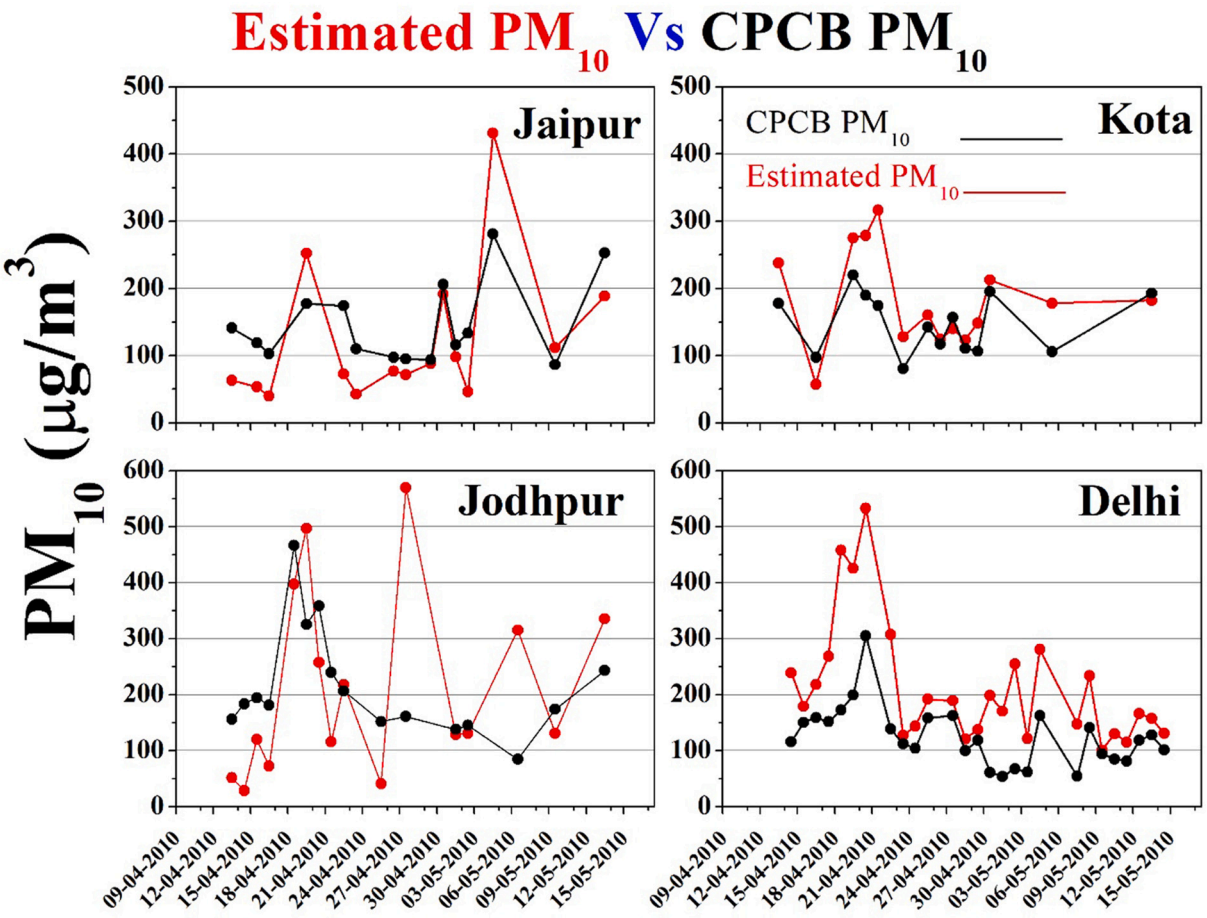

Fig. 6. Estimated PM_{10} against CPCB PM_{10} for Jaipur, Jodhpur, Kota, and Delhi.

Table 3
Summary statistics of slope, intercept, *p*-values and coefficient of determination (R^2).

	Jaipur	Kota	Jodhpur	Delhi	Delhi Dwarka Station
Slope	1.427	1.264	1.785	1.582	1.285
Intercept	−85.970	−3.498	−63.693	15.968	26.109
R^2	0.662	0.600	0.492	0.603	0.681
p value	0.095	0.008	0.023	0.000	0.000

high PM areas correlated well with the areas of high AOD when model outputs are matched within ±00:30 h during satellite overpass time. Model outputs of AOD at Jaipur, Jodhpur, Kota, and Delhi are generally underestimated when compared with MODIS satellite AOD retrievals by around 37%. Some areas were showing low PM_{10} or low dust emissions, the possible reason can be uncertainties in anthropogenic aerosol emissions (e.g., Cherian et al., 2012; Nair et al., 2012). Kumar et al., 2014 shows that during April dust event were generated due to the low-pressure area at Indo Gangetic Plains. This also has caused high surface winds. The spatial correlation of MODIS (Terra and Aqua) with estimated PM_{10} is in the range of 0.26–0.58 for 17^{th}-$22n^{d}$ April 2010 event and 0.26–0.60 for 05^{th}-10^{th} May 2010. The average PBL height during these events is in the range of 1500–3500 m. The PBL height and surface wind comparision shows overestimation by model which caused well mixing and thus lower concentration of aerosols. The point data validation suggested that the events are well correlated and able to capture the trend with CPCB observations of PM_{10}. Correlation of 0.81, 0.70, 0.77 and 0.78 are found respectively for Jaipur, Jodhpur, Kota, and Delhi. In the same way correlation of 0.83 is found for Delhi when hourly observations are matched between CPCB and Estimated PM_{10}. The status of air quality during these events vary from moderately polluted to severe. If prolonged this can cause serious health impacts and increase mortality. AIRS data of dust score > 380 also suggested certainity of dust during these events with more severe scores >450 over parts of Rajasthan, Delhi, IGP region, some parts of punjab during these events.

The WRF-Chem model underestimates AOD. However, if latest emission inventories are there at high resolution than close real

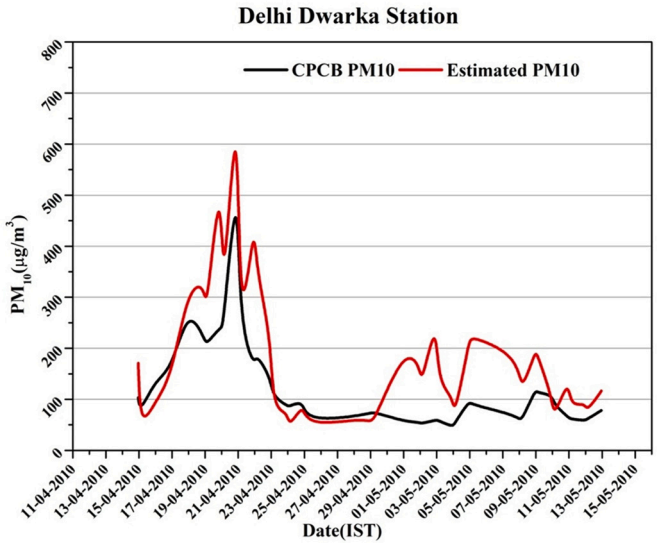

Fig. 7. Graph showing the validation of Estimated PM_{10} against CPCB PM_{10} for Delhi Dwarka station (Estimated Values are taken at 11:00 am and 02:00 pm).

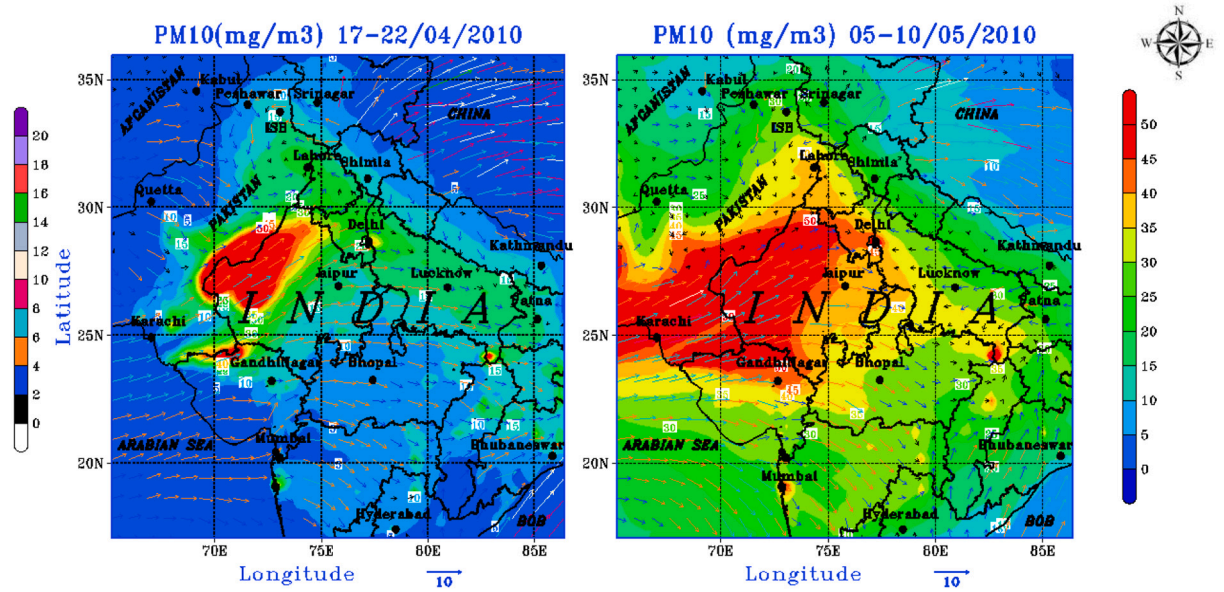

Fig. 8. Total pollution load(PM_{10}) during the peak of events (a) 17th-22nd April 2010 (b) 05th-10th May 2010 (Dust storm). The color bar on the rights shows PM_{10} total in micrograms/cubic meter.

events can be captured. It can be concluded that if more ground station of pollution measuring sites are there then the bias can be estimated at more locations. This, in turn, can improve the scaling and better estimation of particulate pollution.

CRediT authorship contribution statement

Manish Soni: Data Curation, Formal analysis, Validation, Visualisation, Software, Writing - original draft, Writing - review & editing. **Sunita Verma**: Methodology, Validation, Writing – review & editing, Visualization, Writing – original draft. **Manoj K.Mishra**: Methodology, Resources. **R.K. Mall**: Formal Analysis, Writing - review & editing. **Swagata Payra**: Conceptualization, Investigation, Supervision, Software, Writing - review & editing.

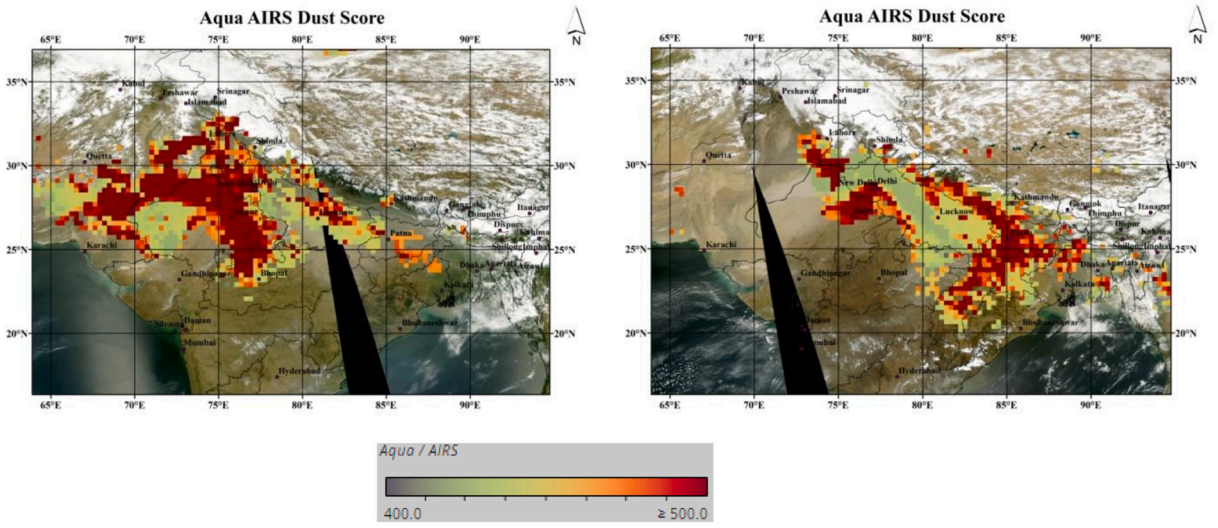

Fig. 9. Dust score using AIRS Level 2.0 V 7.0 data on (a) 20th April 2010 (b) 21st April 2010 (Dust storm). The legend on the right shows when values > 380. There is more certainity of dust.

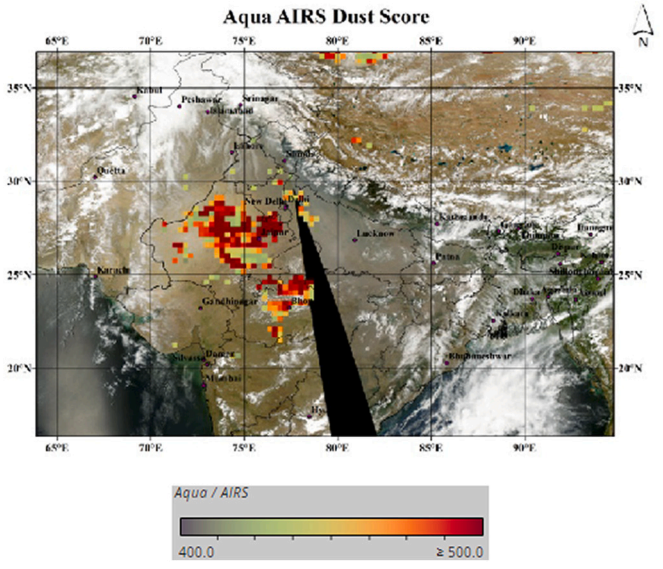

Fig. 10. Dust score using AIRS Level 2.0 V 7.0 data on 03th May 2010 (Dust storm). The legend on the right shows when values > 380. There is more certainity of dust.

Declaration of Competing Interest

We don't have any conflict of interest.

Acknowledgments

MODIS data were obtained from the Level 3 and Atmosphere Archive and Distribution System (LAADS) at Goddard Space Flight Center (GSFC), (http://ladsweb.nascom.nasa.gov/data/). We also acknowledge the MODIS mission scientists, associated NASA personnel and bhuvan portal for supplying AwiFS satellite data in this research effort. We also acknowledge http://wunderground.com, Rajasthan Pollution Control Board, Central Pollution Control Board for providing the meteorological and PM_{10} data. We also like to acknowledge BIT Mesra Jaipur campus and BISR for providing the infrastructure and computing facilities to carry out the research work. The authors gratefully acknowledge the NOAA Air Resources Laboratory (ARL) for the provision of the HYSPLIT transport and dispersion model and/or READY website (https://www.ready.noaa.gov) used in this publication. The authors would

also like to thank funding support from Indian Space Research Organisation under Respond program (ISRO/RES/3/806/19-20).

References

AIRS Science Team/Joao Teixeira, 2013. AIRS/Aqua L2 Support Retrieval (AIRS-only) V006. Goddard Earth Sciences Data and Information Services Center (GES DISC), Greenbelt, MD, USA. https://doi.org/10.5067/Aqua/AIRS/DATA208. Accessed: [Data Access Date].

Beljaars, A.C.M., 1994. The parameterization of surface fluxes in large-scale models under free convection. Quart. J. Roy. Meteor. Soc. 121, 255–270.

Bilal, M., Nichol, J.E., Spak, S.N., 2017. A new approach for estimation of fine particulate concentrations using satellite aerosol optical depth and binning of meteorological variables. Aerosol Air Qual. Res. 17, 356–367.

Chate, D.M., Devara, P.C.S., 2005. Parametric study of scavenging of atmospheric aerosols of various chemical species during thunderstorm and non-thunderstorm rain events. J. Geophys. Res. 110, D23208.

Chen, F., Dudhia, J., 2001. Coupling an advanced land-surface/hydrology model with the Penn State/ NCAR MM5 modeling system. Part I: model description and implementation. Mon. Wea. Rev. 129, 569–585.

Cherian, R., Venkataraman, C., Ramachandran, S., Quaas, J., Kedia, S., 2012. Examination of aerosol distributions and radiative effects over the bay of Bengal and the Arabian Sea region during ICARB using satellite data and a general circulation model. Atmos. Chem. Phys. 12, 1287–1305. https://doi.org/10.5194/acp-12-1287-2012.

Chin, M., Ginoux, P., Kinne, S., Holben, B.N., Duncan, B.N., Martin, R.V., Logan, J.A., Higurashi, A., Nakajima, T., 2002. Tropospheric aerosol optical thickness from the GOCART model and comparisons with satellite and sunphotometer measurements. J. Atmos. Sci. 59, 461–483.

Chinnam, N., Dey, S., Tripathi, S.N., Sharma, M., 2006. Dust events in Kanpur, northern India: chemical evidence for source and implications to radiative forcing. Geophys. Res. Lett. 33, L08803. https://doi.org/10.1029/2005GL025278.

Chitranshi, S., Sharma, S.P., Dey, S., 2015. Satellite-based estimates of outdoor particulate pollution (PM10) for Agra City in northern India. Air Qual. Atmos. Health 8 (1), 55–65.

Chu, D.A., Kaufman, Y.J., Ichoku, C., Remer, L.A., Tanré, D., Holben, B.N., 2002. Validation of MODIS aerosol optical depth retrieval over land. Geophys. Res. Lett. 29, 1617–1620. https://doi.org/10.1029/2001GL013205.

Crippa, P., Sullivan, R.C., Thota, A., Pryor, S.C., 2016. Evaluating the skill of high-resolution WRF-Chem simulations in describing drivers of aerosol direct climate forcing on the regional scale. Atmos. Chem. Phys. 16 (1), 397–416.

Dentener, F.J., Carmichael, G.R., Zhang, Y., Lelieveld, J., Crutzen, P.J., 1996. Role of mineral aerosol as a reactive surface in the global troposphere. J. Geophys. Res. 101, 22869–22889.

Dey, S., Di Girolamo, L., van Donkelaar, A., Tripathi, S.N., Gupta, T., Mohan, M., 2012. Variability of outdoor fine particulate (PM2. 5) concentration in the Indian Subcontinent: A remote sensing approach. Remote Sens. Environ. 127, 153–161.

Dey, S., Tripathi, S.N., Singh, R.P., Holben, B.N., 2004. Influence of dust storms on aerosol opticalproperties over the Indo-Gangetic basin. J. Geophys. Res. 109, D20211. https://doi.org/10.1029/2004JD004924.

Eck, T.F., Holben, B.N., Dubovik, O., Smirnov, A., Slutsker, I., Lobert, J.M., Ramanathan, V., 2001. Column-integrated aerosol optical properties over the Maldives during the northeast monsoon for 1998–2000. J. Geophys. Res. Atmos. 106, 28.

El-Askary, H., Gautam, R., Singh, R., Kafatos, M., 2006. Dust storms detection over the indo-Gangetic Basin using multi sensor data. Adv. Space Res. 37, 728–733. https://doi.org/10.1016/j.asr.2005.03.134.

Fast, J.D., Gustafson Jr., W.I., Easter, R.C., Zaveri, R.A., Barnard, J.C., Chapman, E.G., Grell, G.A., 2006. Evolution of ozone, particulates, and aerosol direct forcing in an urban area using anew fully-coupled meteorology, chemistry, and aerosol model. J. Geophys. Res. 111, D21305. https://doi.org/10.1029/2005JD006721.

Gautam, R., Liu, Z., Singh, R.P., Hsu, N.C., 2009. Two contrasting dust-dominant periods over India observed from MODIS and CALIPSO data. Geophys. Res. Lett. 36, L06813. https://doi.org/10.1029/2008GL036967.

Gharai, B., Rao, P.V.N., Dutt, C.B.S., 2018. Mesoscale model compatible IRS-P6 AWiFS-derived land use/land cover of Indian region. Curr. Sci. 115 (12), 2301–2306.

Ghude, S.D., Pfister, G.G., Jena, C., van der A, R.J., Emmons, L.K., Kumar, R., 2013. Satellite constraints of nitrogen oxide (NOx) emissions from India based on OMI observations and WRF-Chem simulations. Geophys. Res. Lett. 40 (2), 423–428. https://doi.org/10.1002/grl.50065.

Ginoux, P., Chin, M., Tegen, I., Prospero, J.M., Holben, B., Dubovik, O., Lin, S.J., 2001. Sources and distributions of dust aerosols simulated with the GOCART model. J. Geophys. Res.-Atmos. 106, 20255–20273.

Govardhan, G., Nanjundiah, R.S., Satheesh, S.K., Krishnamoorthy, K., Kotamarthi, V.R., 2015. Performance of WRF-Chem over Indian region: comparison with measurements. J. Earth Syst. Sci. 124 (4), 875–896.

Grell, G.A., Peckham, S.E., Schmitz, R., McKeen, S.A., Frost, G., Skamarock, W.C., Eder, B., 2005. Fully coupled "online" chemistry within the WRF model. Atmos. Environ. 39, 6957–6975.

Guenther, A., Karl, T., Harley, P., Wiedinmyer, C., Palmer, P.I., Geron, C., 2006. Estimates of global terrestrial isoprene emissions using MEGAN (Model of Emissions of Gases and Aerosols from Nature). Atmos. Chem. Phys. 6, 3181–3210. https://doi.org/10.5194/acp-6-3181-2006.

Gupta, P., Christopher, S.A., 2009. Particulate matter air quality assessment using integrated surface, satellite, and meteorological products: 2. A neural network approach.J. Geophys. Res. Atmos. 114 (D20).

Gupta, P., Christopher, S.A., Wang, J., Gehrig, R., Lee, Y.C., Kumar, N., 2006. Satellite remote sensing of particulate matter and air quality assessment over global cities. Atmos. Environ. 40 (30), 5880–5892.

Han, X., Zhang, M., Han, Z., Xin, J., Liu, X., 2011. Simulation of aerosol direct radiative forcing with RAMSCMAQ in East Asia. Atmos. Environ. 45 (6576–6592), 2011. https://doi.org/10.1016/j.atmosenv.2011.08.006.

Hegde, P., Pant, P., Naja, M., Dumka, U.C., Sagar, R., 2007. South Asian dust episode in June 2006: aerosol observations in the Central Himalayas. Geophys. Res. Lett. 34, 2007. https://doi.org/10.1029/2007GL030692. L23802.

Hoff, R.M., Christopher, S.A., 2009. Remote sensing of particulate pollution from space: have we reached the promised land? J. Air Waste Manage. Assoc. 59 (6), 645–675.

Hong, S.Y., Noh, Y., Dudhia, J., 2006. A new vertical diffusion package with an explicit treatment of entrainment processes. Mon. Wea. Rev. 134 (9), 2318–2341.

Janssens-Maenhout, G., Dentener, F., Van Aardenne, J., Monni, S., Pagliari, V., Orlandini, L., Keating, T., 2012. EDGAR-HTAP: a harmonized gridded air pollution emission dataset based on national inventories, 25229. European Commission Publications Office, Ispra, Italy, p. 40.

Jickells, T.D., An, Z.S., Andersen, K.K., Baker, A.R., Bergametti, G., Brooks, N., Cao, J.J., Boyd, P.W., Duce, R.A., Hunter, K.A., Kawahata, H., Kubilay, N., la Roche, J., Liss, P.S., Mahowald, N., Prospero, J.M., Ridgwell, A.J., Tegen, I., Torres, R., 2005. Global iron connections between desert dust, ocean biogeochemistry and climate. Science 308, 67–71.

Kain, J.S., 2004. The Kain–Fritsch convective parameterization: an update. J. Appl. Meteorol. Climatol. 43 (1), 170–181.

Kalenderski, S., Stenchikov, G., Zhao, C., 2013. Modeling a typical winter-time dust event over the Arabian Peninsula and the Red Sea. Atmos. Chem. Phys. 13, 1999–2014. https://doi.org/10.5194/acp-13-1999-2013.

Kaufman, Y.J., Tanre, D., Remer, L.A., Vermote, E.F., Chu, A., Holben, B.N., 1997. Operational remote sensing of tropospheric aerosol over land from EOS moderate resolution imaging spectroradiometer. J. Geophys. Res. 102, 17051–17067.

Kim, K., Lee, K.H., Kim, J.I., Noh, Y., Shin, D.H., Shin, S.K., Lee, D., Kim, J., Kim, Y.J., Song, C.H., 2016. Estimation of surface-level PM concentration from satellite observation taking into account the aerosol vertical profiles and hygroscopicity. Chemosphere 143, 32–40.

Koelemeijer, R.B.A., Homan, C.D., Matthijsen, J., 2006. Comparison of spatial and temporal variations of aerosol optical thickness and particulate matter over Europe. Atmos. Environ. 40 (27), 5304–5315. https://doi.org/10.1016/j.atmosenv.2006.04.044.

Kondragunta, S., Lee, P., McQueen, J., Kittaka, C., Prados, A.I., Ciren, P., Laszlo, I., Pierce, R.B., Hoff, R., Szykman, J.J., 2008. Air quality forecast verification using satellite data. J. Appl. Meteorol. Climatol. 47, 425–442.

Krishna, R.K., Ghude, S.D., Kumar, R., Beig, G., Kulkarni, R., Nivdange, S., Chate, D., 2019. Surface PM2. 5 estimate using satellite-derived aerosol optical depth over India. Aerosol Air Qual. Res. 19 (1), 25–37.
Kumar, R., Naja, M., Pfister, G.G., Barth, M.C., Brasseur, G.P., 2012a. Simulations over South Asia using the weather research and forecasting model with chemistry (WRF-Chem): set-up and meteorological evaluation. Geosci. Model Dev. 5, 321–343. https://doi.org/10.5194/gmd-5-321-2012.
Kumar, R., Naja, M., Pfister, G.G., Barth, M.C., Wiedinmyer, C., Brasseur, G.P., 2012b. Simulations over South Asia using the weather research and forecasting model with chemistry (WRF-Chem):chemistry evaluation and initial results. Geosci. Model Dev. 5, 619–648. https://doi.org/10.5194/gmd-5-619-2012.
Kumar, R., Barth, M.C., Pfister, G.G., Naja, M., Brasseur, G.P., 2014. WRF-Chem simulations of a typical pre-monsoon dust storm in northern India: influences on aerosol optical properties and radiation budget. Atmos. Chem. Phys. 14 (5), 2431–2446.
Lee, H.J., Liu, Y., Coull, B.A., Schwartz, J., Koutrakis, P., 2011. A novel calibration approach of MODIS AOD data to predict PM2. 5 concentrations. Atmos. Chem. Phys. 11 (15), 7991.
Levy, R.C., Remer, L.A., Mattoo, S., Vermote, E.F., Kaufman, Y.J., 2007. Second-generation operational algorithm: retrieval of aerosol properties over land from inversion of moderate resolution imaging Spectroradiometer spectral reflectance. J. Geophys. Res. 112, D13. https://doi.org/10.1029/2006JD007811.
Li, F., Ginoux, P., Ramaswamy, V., 2008. Distribution, transport, and deposition of mineral dust in the Southern Ocean and Antarctica: contribution of major sources. J. Geophys. Res. 113, D10207. https://doi.org/10.1029/2007JD009190.
Li, R., Gong, J., Chen, L., Wang, Z., 2015. Estimating ground-level PM2.5 using fine-resolution satellite data inthe megacity of Beijing, China. Aerosol Air Qual. Res. 15, 1347–1356.
Lin, C., Li, Y., Yuan, Z., Lau, A.K., Li, C., Fung, J.C., 2015. Using satellite remote sensing data to estimate the high-resolution distribution of ground-level PM2.5. Remote Sens. Environ. 156, 117–128.
Liu, Y., Park, R.J., Jacob, D.J., Li, Q., Kilaru, V., Sarnat, J.A., 2004. Mapping annual mean ground-level PM2.5 concentrations using multiangle imaging Spectroradiometer aerosol optical thickness over thecontiguous United States. J. Geophys. Res. 109, D22206.
Liu, Y., Sarnat, J.A., Kilaru, V., Jacob, D.J., Koutrakis, P., 2005. Estimating ground-level PM2.5 eastern United States using satellite remote sensing. Environ. Sci. Technol. 39, 3269–3278.
Liu, Y., Franklin, M., Kahn, R., Koutrakis, P., 2007. Using aerosol optical thickness to predict ground-level PM 2.5 concentrations in the St. Louis area: a comparison between MISR and MODIS. Remote Sens. Environ. 107, 33–44.
Mahowald, N.M., Baker, A.R., Bergametti, G., Brooks, N., Duce, R.A., Jickells, T.D., Kubilay, N., Prospero, J.M., Tegen, I., 2005. Atmospheric global dust cycle and iron inputs to the ocean. Global Biogeochem. Cy. 19 https://doi.org/10.1029/2004GB002402. GB4025.
Miller, R.L., Tegen, I., Perlwitz, J., 2004. Surface radiative forcing by soil dust aerosols and the hydrologic cycle. J. Geophys. Res. 109, D04203. https://doi.org/10.1029/2003JD004085.
Mlawer, E.J., Taubman, S.J., Brown, P.D., Iacono, M.J., Clough, S.A., 1997. Radiative transfer for inhomogeneous atmospheres: RRTM, a validated correlated-k model for the longwave. J. Geophys. Res. Atmos. 102 (D14), 16663–16682.
Moorthy, K.K., Babu, S.S., Satheesh, S.K., Srinivasan, J., Dutt, C.B.S., 2007. Dust absorption over the "Great Indian Desert" inferred using ground-based and satellite remote sensing. J. Geophys. Res. Atmos. 112 (D9).
Nair, V.S., Solmon, F., Giorgi, F., Mariotti, L., Babu, S.S., Moorthy, K.K., 2012. Simulation of South Asian aerosols for regional climate studies. J. Geophys. Res. 117, D04209. https://doi.org/10.1029/2011JD016711.
Pandithurai, G., Dipu, S., Dani, K.K., Tiwari, S., Bisht, D.S., Devara, P.C.S., Pinker, R.T., 2008. Aerosol radiative forcing during dust events over New Delhi, India. J. Geophys. Res. 113, D13209. https://doi.org/10.1029/2008JD009804.
Park, M.E., Song, C.H., Park, R.S., Lee, J., Kim, J., Lee, S., Woo, J.H., Carmichael, G.R., Eck, T.F., Holben, B.N., Lee, S.S., 2014. New approach to monitor transboundary particulate pollution over Northeast Asia. Atmos. Chem. Phys. 14 (2), 659–674.
Payra, S., Soni, M., Kumar, A., Prakash, D., Verma, S., 2015. Intercomparison of aerosol optical thickness derived from MODIS and in situ ground datasets over Jaipur, a semiarid zone in India. Environ. Sci. Technol. 49 (15), 9237–9246.
Pfister, G.G., Parrish, D.D., Worden, H., Emmons, L.K., Edwards, D.P., Wiedinmyer, C., Diskin, G.S., Huey, G., Oltmans, S.J., Thouret, V., Weinheimer, A., Wisthaler, A., 2011. Characterizing summertime chemical boundary conditions for airmasses entering the US West Coast. Atmos. Chem. Phys. 11, 1769–1790. https://doi.org/10.5194/acp-11-1769-2011.
Prasad, A.K., Singh, R.P., 2007. Changes in aerosol parameters during major dust storm events (2001–2005) over the Indo-Gangetic Plains using AERONET and MODIS data. J. Geophys. Res. 112, D09208. https://doi.org/10.1029/2006JD007778.
Prasad, A.K., Singh, S., Chauhan, S.S., Srivastava, M.K., Singh, R.P., Singh, R., 2007. Aerosol radiative forcing over the indo-Gangetic Plains during major storms. Atmos. Environ. 41, 6289–6301.
Prospero, J.M., Lamb, J.P., 2003. African droughts and dust transport to the Caribbean: climate change and implications. Science 302, 1024–1027.
Prospero, J.M., Ginoux, P., Torres, O., Nicholson, S.E., Gill, T.E., 2002. Environmental characterization of global sources of atmospheric soil dust identified with the Nimbus 7 Total ozone Mapping Spectrometer (TOMS) absorbing aerosol product. Rev.Geophys. 40, 1002. https://doi.org/10.1029/2000RG000095.
Remer, L.A., Kaufman, Y.J., Tanré, D., Mattoo, S., Chu, D.A., Martins, J.V., Li, R.R., Ichoku, C., Levy, R.C., Kleidman, R.G., Eck, T.F., 2005. The MODIS aerosol algorithm, products, and validation. J. Atmos. Sci. 62, 947–973. https://doi.org/10.1175/JAS3385.1.
Satheesh, S.K., Srinivasan, J., 2002. Enhanced aerosol loading over Arabian Sea during the pre-monsoon season: natural or anthropogenic? Geophys. Res. Lett. 29 (18), 21–1.
Sharma, D., Singh, D., Kaskaoutis, D.G., 2012. Impact of two intense dust storms on aerosol characteristics and radiative forcing over Patiala, northwestern India. Adv. Meteorol. 2012 https://doi.org/10.1155/2012/956814, 956814.
Sikka, D.R., 1997. Desert climate and its dynamics. Curr. Sci. 35–46.
Skamarock, W.C., Klemp, J.B., Dudhia, J., Gill, D.O., Barker, D.M., Wang, W., Powers, J.G., 2008. A Description of the Advanced Research WRF Version 2. NCAR Tech. Note, NCAR/TN-468+STR. Natl. Cent. for Atmos. Res., Boulder, CO. available at: http://wrf-model.org/wrfadmin/publications.php.
Song, W., Jia, H., Huang, J., Zhang, Y., 2014. A satellite-based geographically weighted regression model for regional PM 2.5 estimation over the Pearl River Delta region in China. Remote Sens. Environ. 154, 1–7.
Soni, M., Payra, S., Verma, S., 2018. Particulate matter estimation over a semi arid region Jaipur, India using satellite AOD and meteorological parameters. Atmos. Pollut. Res. https://doi.org/10.1016/j.apr.2018.03.001.
Sotoudeheian, S., Arhami, M., 2014. Estimating ground-level PM10 using satellite remote sensing and ground-based meteorological measurements over Tehran. J. Environ. Health Sci. Eng. 12 (1), 122.
Tegen, I., Fung, I., 1994. Modeling of mineral dust in the atmosphere: sources, transport, and optical thickness. J. Geophys. Res. 99, 22897–22914. https://doi.org/10.1029/94JD01928.
Teller, A., Xue, L., Levin, Z., 2012. The effects of mineral dust particles, aerosol regeneration and ice nucleation parameterizations on clouds and precipitation. Atmos. Chem. Phys. 12, 9303–9320. https://doi.org/10.5194/acp-12-9303-2012.
Thompson, G., Rasmussen, R.M., Manning, K., 2004. Explicit forecasts of winter precipitation using an improved bulk microphysics scheme. Part I: description and sensitivity analysis. Mon. Wea. Rev. 132 (2), 519–542.
Uno, I., Wang, Z., Chiba, M., Chun, Y.S., Gong, S.L., Hara, Y., Jung, E., Lee, S.S., Liu, M., Mikami, M., Music, S., Nickovic, S., Satake, S., Shao, Y., Song, Z., Sugimoto, N., Tanaka, T., Westphal, D.L., 2006. Dust model intercomparison (DMIP) study Over Asia: overview. J. Geophys. Res.-Atmos. 111, D12213. https://doi.org/10.1029/2005JD006575.
Van Donkelaar, A., Martin, R.V., Park, R.J., 2006. Estimating ground-level PM2.5 using aerosol opticaldepth determined from satellite remote sensing. J. Geophys. Res. 111, D21201.
Van Donkelaar, A., Martin, R.V., Brauer, M., Kahn, R., Levy, R., Verduzco, C., Villeneuve, P.J., 2010. Global estimates of ambient fine particulate matter concentrations from satellite-based aerosol optical depth:Development and application. Environ. Health Perspect. 118, 847.

Wang, K., Zhang, Y., Nenes, A., Fountoukis, C., 2012. Implementation of dust emission and chemistry into the Community Multiscale Air Quality modeling system and initial application to an Asian dust storm episode. Atmos. Chem. Phys. 12, 10209–10237. https://doi.org/10.5194/acp-12-10209-2012.

Washington, R., Todd, M., Middleton, N.J., Goudie, A.S., 2003. Dust storm source areas determined by the Total ozone monitoring spectrometer and surface observations. Ann. Assoc. Am. Geogr. 93 (297–313), 2003.

Wiedinmyer, C., Akagi, S.K., Yokelson, R.J., Emmons, L.K., Al-Saadi, J.A., Orlando, J.J., Soja, A.J., 2011. The Fire Inventory from NCAR (FINN): a high resolution global model to estimate the emissions from open burning. Geosci. Model Dev. 4, 625–641. https://doi.org/10.5194/gmd-4-625-2011.

Yao, Zhigang, Li, Jun, Zhao, Zengliang, Zhu, Lin, Qi, Jin, Che, Huizheng, 2019. Extracting taklimakan dust parameters from AIRS with Artificial neural network method. Remote Sens. 11 (24), 2931. https://doi.org/10.3390/rs11242931.

Yap, X.Q., Hashim, M., 2013. A robust calibration approach for PM10 prediction from MODIS aerosol optical depth. Atmos. Chem. Phys. 13, 3517–3526. https://doi.org/10.5194/acp-13-3517-2013.

Zhang, Z.H., Hu, M.G., Ren, J., Zhang, Z.Y., Christakos, G., Wang, J.F., 2017. Probabilistic assessment of high concentrations of particulate matter (PM 10) in Beijing, China. Atmos. Poll. Res. https://doi.org/10.1016/j.apr.2017.04.006.

Zhao, C., Liu, X., Leung, L.R., Johnson, B., McFarlane, S.A., Gustafson Jr., W.I., Fast, J.D., Easter, R., 2010. The spatial distribution of mineral dust and its shortwave radiative forcing over North Africa: modeling sensitivities to dust emissions and aerosol size treatments. Atmos. Chem. Phys. 10, 8821–8838. https://doi.org/10.5194/acp-10-8821-2010.

Zhao, C., Liu, X., Ruby Leung, L., Hagos, S., 2011. Radiative impact of mineral dust on monsoon precipitation variability over West Africa. Atmos. Chem. Phys. 11, 1879–1893. https://doi.org/10.5194/acp-11-1879-2011.